

## Chlorinated Polyethylene. III. Relationships of Microstructure and Thermal Properties

Bienvenu-Magloire QUENUM, Philippe BERTICAT, and Georges VALLET

*Laboratoire de Chimie Macromoléculaire, Université Claude Bernard  
43, Boulevard du 11 Novembre 1918-69621 Villeurbanne, France.*

(Received June 17, 1974)

**ABSTRACT:** The thermal properties (*viz.*, second-order transitions, melting points, dynamic and isothermal heat behaviour) of chlorinated polyethylene (CPE) samples are studied here. Thermomechanical analysis (TMA), differential thermal analysis (DTA), and thermogravimetric analysis (TGA) results are listed together to correlate the thermal properties and the microstructure of CPE samples, of various chlorine contents by weight, produced from thermal chlorinated or photochlorinated linear and branched polyethylene samples. The dehydrochlorination rate of a CPE sample is shown to be strongly dependent on its microtacticity up to a 56–61-% chlorine content by weight value. Beyond this 56–61-%Cl<sub>2</sub> interval the microtacticity influence is screened by the steric hindrance introduced by the  $\alpha_{\text{I}}$  ( $-\text{CH}_2-\text{CHCl}-\text{CCl}_2-$  or  $-\text{CHCl}-\text{CHCl}-\text{CCl}_2-$ ),  $\alpha_{\text{II}}$   $-\text{CHCl}-\text{CHCl}-\text{CHCl}-$  or  $-\text{CH}_2-\text{CHCl}-\text{CHCl}-$ , and  $\beta_{\text{II}}$  ( $-\text{CHCl}-\text{CH}_2-\text{CCl}_2-$ ) structures. At the saturation level (73-% Cl<sub>2</sub>), the higher a CPE ratio, nb CHCl/nb CH<sub>2</sub>, is, the lower is its maximum dehydrochlorination rate. When its ratio, nb<sup>2</sup> CHCl/nb CH<sub>2</sub>, is less than 4, a saturated (73%) CPE sample has a unique global dehydrochlorination activation energy ( $E_a$ ); when this ratio stands between 4 and 6, there are two global dehydrochlorination  $E_a$ . The structures which could be regarded as responsible for these different global  $E_a$  and the second-order transitions are specified.

**KEY WORDS** Chlorinated Polyethylene / Thermomechanical Analysis / Differential Thermal Analysis / Thermogravimetric Analysis / Second-Order Transitions / Maximum Dehydrochlorination Rate /

Very few studies have been published about the thermal properties of CPE. The first one, made by Oswald and Kubu<sup>1</sup> dealt with glass-transition temperatures ( $T_g$ ). Erä and Lindberg<sup>2</sup> showed the effect of heat treatment on crystallinity. Abu Isa<sup>3</sup> studied the dechlorination mechanism and the effect of added antimony oxide on the rate of dehydrochlorination. Saglio, *et al.*,<sup>4</sup> studied the degradation of saturated (73%) CPE and showed that fibers of saturated CPE can be used as a carbon fiber precursor.

The CPE samples used for the above studies were, generally, commercial ones supplied without the specific conditions of their preparation which are required<sup>5</sup> to correlate microstructure and properties. In addition, their microstructural characterizations have been made only with infrared analysis, which is not sufficient.

Since we have prepared and characterized various CPE samples<sup>5–10</sup> we will be able to cor-

relate their microstructure and thermal properties in this paper.

In carbon backbone high polymers secondary transitions can be detected besides the main second-order transition, *i.e.*, the glass-transition temperature ( $T_g$ ), and the main first-order transition, *i.e.* the solid-liquid-transition or the melting temperature. They are:

(1) The secondary second-order transitions occurring, generally, at temperatures less than  $T_g$ . They are related to the motion of short segments of the polymer's backbone (*viz.*, branchings, substituents, "crankshaft" or "kink" mechanisms<sup>11,12</sup>) related to motions in the amorphous or crystalline phase.

(2) The secondary first-order transition or crystal—crystal transition which involves changes of crystalline forms. We will not take into account this secondary first-order transition because the crystallinity of the polyethylene is rapidly

reduced as the chlorination proceeds.

## EXPERIMENTAL

### Materials

Two kinds of CPE samples have been employed:

Those of chlorine contents by weight less than 73-%  $\text{Cl}_2$ : *i.e.*, branched polyethylene samples photochlorinated at 20°C in 1,1,2,2-tetrachloroethane (TCE) (type Ia); branched polyethylene samples thermally chlorinated at 90°C in TCE (type Ib); linear polyethylene samples thermally chlorinated at 110°C in TCE (type Ic).<sup>5</sup>

Those chlorinated at saturation level (73-%  $\text{Cl}_2$ ): *i.e.*, branched polyethylene samples (type IIa) and linear polyethylene samples (type IIa') photochlorinated at 20°C in carbon tetrachloride ( $\text{CCl}_4$ ) during 4–6–8 hr;<sup>7</sup> branched polyethylene samples (type IIb) and linear polyethylene samples (type IIb') photochlorinated during 4 hr at 20°C; 40°C; 60°C<sup>8</sup> in  $\text{CCl}_4$ .

### Second-Order Transitions

The Dupont 942 Thermomechanical Analyser (942 TMA), coupled with the 990 Dupont Recorder was used to detect the second-order transitions of the CPE samples of type I. The experimental samples were the CPE-films describes previously.<sup>6</sup> The tension-probe technique was used to record the changes of the elastic modulus of the CPE-film under a load, as a function of rising temperature. This technique is accurate only if the applied load does not cause any creep of the experimental sample in the time-frame of the experiment, *i.e.*, in the temperature interval investigated. For all the measurements the experimental samples were 13 mm long (between two cleaved lead balls) and 2 mm wide; the applied load was 2 g and the heating rate was 5°C/min from a 40°C starting temperature.

### Melting Temperatures

The Dupont 990 Thermal Analyser, coupled with the "DSC cell," was used to detect the melting points of the CPE samples of type I. Quantities of 5–10 mg of the powdered sampled were used. The heating rate was 10°C/min from room temperature (23°C). All the measurements were conducted in helium atmosphere.

### Thermogravimetric Studies

A Cahn electrobalance Model R-H transformed

into a TGA-instrument was used (Figure 1).

The glass wares were made from quartz. Each oven had an electric power of 1100 W. The temperature-regulation device was a Stanton

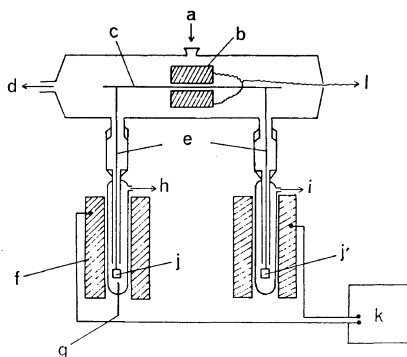


**Figure 1.** TGA apparatus: a, inert gas inlet; b, magnet; c, beam; d, vacuum system; e, hanging; f, oven; g, measurement thermocouple; h, gas outlet; i, inert gas outlet; j, sample holder; j', reference sample holder; k, regulation system; l, recorder device.

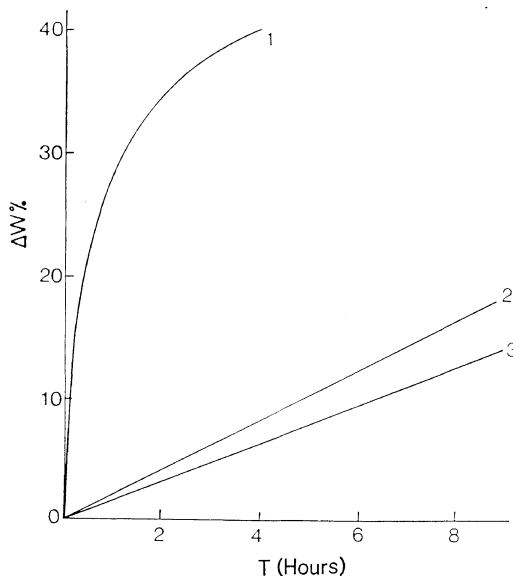


**Figure 2.** Isothermal (235°C) TGA. Influence of the molecular-weight distribution (MWD) of a 73-% CPE sample upon its weight-loss magnitude: 1, lowest number-average molecular weight,  $L\bar{M}_n$ , 6000; 2 medium number-average molecular weight,  $M\bar{M}_n$ , 15000; (3) highest number-average molecular weight,  $H\bar{M}_n$ , 50000.

redcroft's model; the recorder was a Kipp—Zonen Model BD-5.

We used the TGA dynamic method, *i.e.*, the recording of the weight loss as the temperature is raised at a constant rate ( $2^{\circ}\text{C}/\text{min}$ ), to study the thermal behaviour of all the CPE samples (types I and II) over the  $180^{\circ}\text{C}$ — $500^{\circ}\text{C}$  interval. A Cahn Time-Derivative Computer Model MARK II, coupled with the TGA apparatus, was used to record the degradation rate.

The global activation energies ( $E_a$ ) of the dehydrochlorination process have been calculated for the CPE samples of type II, *viz.*, those chlorinated to the saturation level (73-%  $\text{Cl}_2$ ) by using the isothermal method.<sup>13</sup> The polymeric chains' breakages occurring during the chlorination process could be enhanced if the chlorination time exceeds the minimum time necessary to obtain the saturation level.<sup>5,7</sup>

Figure 2 shows the influence of the molecular weight of a saturated (73-%  $\text{Cl}_2$ ) CPE sample upon its weight-loss magnitude in an isothermal process; the fraction of the lowest number-average molecular weight ( $L\bar{M}_n$ ) is rapidly degraded. Thus, to have reproducible runs and comparative results it is necessary to use homogeneous samples. All the experimental CPE samples of type II used in the isothermal process were fractions of the highest number-average molecular weight ( $H\bar{M}_n$ ) obtained by fractionation of the initial samples in a 70/30 mixture of tetrahydrofuran and methyl alcohol at room temperature.<sup>7</sup>

For each experiment, isothermal or dynamic, 20 mg of powdered CPE sample were used. All the experiments were conducted in nitrogen atmosphere; the rate-flow of the gas through the sample and the reference tubes (Figure 1) was 6 l/hr. The heating rate in the dynamic method was  $2^{\circ}\text{C}/\text{min}$ . These experimental conditions which permit reproducible runs, matched those advocated by Wendlandt,<sup>13</sup> Guyot and Bert.<sup>14</sup>

## RESULTS AND DISCUSSION

Two main theories have been established to explain the second-order transitions of polymers and particularly the glass transition: a kinetic based one<sup>12</sup> and a thermodynamical one.<sup>15</sup> In the following discussion we will follow the

kinetic theory.

### Melting Points and Second-Order Transitions

In Table I are listed the results obtained with the DTA experiments; three melting temperatures are reported:  $T_A$  is related to the starting of the melting process and  $T_C$  to its end, *i.e.*, when the disruption of the polyethylene's crystallinities is completed. Many scientists use  $T_{fm}$ , the temperature at the thermogram-top (Figure 3), to characterize fusion. This  $T_{fm}$ -temperature can be related to the average statistical thickness of the crystallites if the thermogram areas, on each side of the  $T_{fm}$ -vertical-line, are symmetrical.

When the thermal chlorination proceeds, the crystallinity of the polyethylene samples (branched or linear) is rapidly destroyed (Table I); the numerous  $-\text{CCl}_2-$  units appearing during the first chlorination step<sup>5</sup> can be regarded as responsible for this. But in the photochlorination process, the CPE samples keep some crystallinity up to a high chlorine-content value by weight; the crystallites disappearance is completed only beyond the 67.5-% chlorine content value, as proved by dynamic mechanical properties studies; the 67.5—73-% photochlorinated CPE samples are amorphous ones, although they are hard and brittle owing to the presence of dichloro and trichloroethylene units.<sup>10</sup>

In Table II are listed the Dupont 942 TMA results (second-order transitions). The asterisked transitions stand between the  $T_A$  and the  $T_C$  (Table I) of the CPE samples and can be related to the motions of short segments of the polymeric chains in the CPE crystalline phase. The

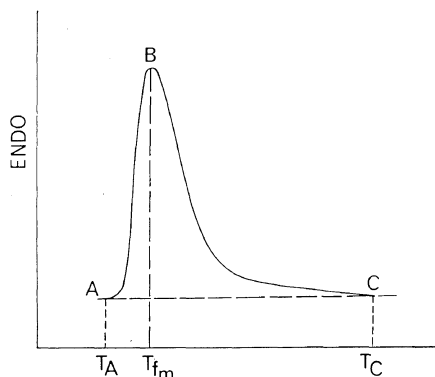


Figure 3. Thermogram of the 6-%  $\text{Cl}_2$  linear CPE sample.

## Chlorinated Polyethylene. III.

 Table I. Melting points of the CPE samples<sup>a</sup>

Type Ia. LDPE photochlorinated at 20°C in TCE					Type Ib. LDPE thermalchlorinated at 90° in TCE					Type Ic. HDPE thermalchlorinated at 110°C in TCE				
T-%, Cl <sub>2</sub>	T <sub>A</sub> , °C	T <sub>f,m</sub> , °C	T <sub>C</sub> , °C	ΔH, cal/g	T-% Cl <sub>2</sub>	T <sub>A</sub> , °C	T <sub>f,m</sub> , °C	T <sub>C</sub> , °C	ΔH, cal/g	T-% Cl <sub>2</sub>	T <sub>A</sub> , °C	T <sub>f,m</sub> , °C	T <sub>C</sub> , °C	ΔH, cal/g
19.5	69	101	112	14.75	24	50	57	72	8.8	6	78.5	81	123.5	39.1
46	82	105	112	11.6	33	32.5	41 61 73	86	—	41	—	—	—	—
55	86	88	112	3.2	54.5	—	—	—	—	56	—	—	—	—
60.5	65.5	82 100	100	—	61.5	—	—	—	—	61.7	—	—	—	—
67.5	—	—	—	—	65	—	—	—	—	64	—	—	—	—
68.4	—	—	—	—	—	—	—	—	—	67	—	—	—	—

<sup>a</sup> The dashed lines indicate that the CPE sample did not show any melting point in the 25–180°C range.

Initial LDPE  $T_{f,m}$ , 110°C;  $\Delta H$ , 32.8 cal/g.

Initial HDPE  $T_{f,m}$ , 134°C;  $\Delta H$ , 58 cal/g.

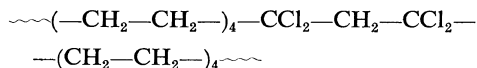
$T_A$ , melting-process starting;  $T_{f,m}$ , temperature at the thermogram-top;  $T_C$ , melting-process end.

The thermograms of the 60.5-% Cl<sub>2</sub> photochlorinated CPE sample and the 33-% Cl<sub>2</sub> thermal chlorinated CPE sample show many  $T_{f,m}$ ; in such cases the calculation of the  $\Delta H$  is not easy.

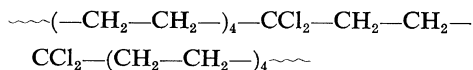
temperatures of nearly all these asterisked transitions are in close agreement with the temperatures of the  $\alpha$ -relaxation peak of the photochlorinated CPE samples.<sup>10</sup>

The other transitions *i.e.*, the non-asterisked ones, can be easily related to the various structures revealed by the microstructural nuclear-magnetic-resonance (NMR) study.<sup>5,9</sup>

In the thermal-chlorination process, between  $\epsilon$ -% Cl<sub>2</sub> and 24-% Cl<sub>2</sub>, the chlorination mechanism is not yet a random one. The —CCl<sub>2</sub>— groups of the structures, such as:



or



are responsible for almost the whole chlorine content value<sup>5</sup> and the thermal CPE samples still keep crystallinity. When the poly(vinyl chloride) (PVC) triads  $\alpha_{\text{III}}$  (—CH<sub>2</sub>—CHCl—CH<sub>2</sub>—) and  $\beta_{\text{III}}$  (—CHCl—CH<sub>2</sub>—CHCl—) appear from the 24-% Cl<sub>2</sub> value) the chlorination mechanism becomes a random one,<sup>5</sup> which destroys the crystallinity of the thermal CPE samples. The numerous —CCl<sub>2</sub>— units along with the few

—CHCl— units behave like a plasticizer, which lowers the second-order transition temperature. This effect is maximum in the range of the 33—41-% chlorine content and the 33—41-% CPE samples are similar to elastomers.<sup>10</sup>

Beyond the 33—41-% Cl<sub>2</sub> range PVC sequences increase and the temperatures of the second-order transitions rise.

When the PVC sequences reach their maximum length, there is an important difference between the 56-% thermal-chlorinated linear polyethylene sample and the 61.5-% thermal-chlorinated branched-polyethylene sample. The latter has more  $\beta'_{\text{IV}}$  structure (mono or dichloropropane or butane); otherwise the 61.5-% thermally chlorinated branched polyethylene sample has PVC sequences shorter than those of the 56-% thermally chlorinated linear polyethylene sample.<sup>5</sup> Thus, at the proper temperature, those short PVC sequences will go easily into motion along with the  $\beta'_{\text{IV}}$  structures and consequently the 61.5-% thermal (branched) CPE sample has a unique second-order transition. On the contrary, the long PVC sequences of the 56-% thermal (linear) CPE sample will not go easily into motion a long with the  $\beta'_{\text{IV}}$  structures; the two entities, the PVC sequences and the  $\beta'_{\text{IV}}$  structures, will each have its second-order transition

temperature, with that of the  $\beta'_{IV}$  structures being lower. As the  $\beta_{II}$  ( $-\text{CHCl}-\text{CH}_2-\text{CHCl}-$ ) structures neighboring with  $\text{CHCl}$  units are already present in large amounts in the 56-% thermal (linear) CPE sample, their second-order transition temperature will take place at a temperature higher than that of the PVC sequences.

In the photochlorination process, when the reaction is carried out in a suspension medium (20°C), the radical substitution of the hydrogen atoms by chlorine atoms starts in the amorphous phase of the polymer and vinyl units first appear.<sup>5</sup> These vinyl units are responsible for a unique second-order transition up to about the

20-% chlorine content. From this value PVDC triads or tetrads ( $-\text{CCl}_2-\text{CH}_2-\text{CCl}_2-$  or  $-\text{CCl}_2-\text{CH}_2-\text{CH}_2-\text{CCl}_2-$ ) appear randomly in the photochlorinated CPE chains.<sup>5</sup> When these PVDC units reach their maximum proportion the photochlorinated CPE samples have two second-order transitions. The short PVC sequences surrounded by a PVDC triad or tetrad can be regarded as responsible for the second-order transition taking place at the lower temperature; the other second-order transition can be attributed to the motion of the long PVC sequences.

In the thermal chlorination process or in the photochlorination one, when the reaction proceeds beyond the 56–61.5-%  $\text{Cl}_2$  range, the  $\alpha_{II}$  ( $-\text{CHCl}-\text{CHCl}-\text{CHCl}-$  or  $-\text{CH}_2-\text{CHCl}-\text{CH}_2-$ ) and the  $\alpha_I$  ( $-\text{CHCl}-\text{CHCl}-\text{CCl}_2-$  or  $-\text{CH}_2-\text{CHCl}-\text{CCl}_2-$ ) structures which appear stiffen the CPE chains;<sup>10</sup> their second-order transition temperatures are distinct and higher than those of the previously described structures.

To sum up, we have reported in Tables Va, Vb and Vc the structures which can be regarded as responsible for the second-order transitions. During the discussion we have not named any of the second-order transitions of CPE sample a glass transition ( $T_g$ ), since the Dupont 942 TMA method is only a qualitative one. But the second-order transitions revealed by the TMA method and those revealed by the dynamic mechanical properties' studies, carried out with the Rheovibron,<sup>10</sup> appear at almost the same temperatures; thus it is easy by listing together the two different results and by defining the  $T_g$  as the temperature for which the complex modulus decreases sharply to identify the  $T_g$ . These are plus-marked in Tables V.

In our previous study<sup>10</sup> we showed that between the 46–60.5% chlorine-content range (for photochlorinated CPE samples) the  $\alpha$ -peak (motions in the crystalline phase of the CPE sample) and the  $\beta$ -peak (vinyl sequences motion) stand at the same temperature. In this chlorine-content interval, the disruption of the crystallites of the polyethylene is high although not yet completed (see Table I). It is important to notice that, in spite of the difference in technique, the Dupont 942 TMA method reveals a similar behavior for the 46–60.6-% photochlorinated CPE

Table II. Second-order transitions of the CPE samples<sup>a</sup>

Type Ia. LDPE photochlorinated at 20°C in TCE <sup>b</sup>					
$T_g$ -% $\text{Cl}_2$	$\frac{\text{CHCl}}{\text{CH}_2}$	$\overline{\text{DP}}_n$	Transition		
			1st	2nd	3rd
16	0.111	1270	36°C	103°C*	—
19.5	—	—	33°C	96°C*	—
46	0.266	1320	48°C	71°C	90°C*
55	0.316	2750	66°C	78°C	—
60.5	0.9	2930	76°C	88°C	—
67.5	1.88	2220	76°C	108°C	148°C
68.4	1.98	700	78°C	137°C	150°C
Type Ib. LDPE thermal-chlorinated at 90°C in TCE <sup>b</sup>					
24	$\epsilon$	1000	32°C	56°C*	—
33	0.07	1580	–12°C	—	—
54.5	0.38	1760	60°C	—	—
61.5	0.44	1310	55°C	—	—
65	1.31	1065	58°C	70°C	102°C
Type Ic. HDPE thermal-chlorinated at 110°C in TCE <sup>b</sup>					
6	$\epsilon$	1500	10°C	104°C*	—
41	0.114	1810	0°C	—	—
56	0.483	1360	52°C	68°C	90°C
61.7	1.27	1000	76°C	94°C	130°C
64	1.975	595	80°C	128°C	160°C
67	2.66	328	75°C	160°C	176°C

<sup>a</sup> The starting temperature was –40°C; the initial HDPE has a unique second-order transition temperature at 12°C, and the initial LDPE one at –20°C.

<sup>b</sup> TCE, 1,1,2,2-tetrachloroethane.

samples (e.g., the 55-% CPE samples in Table Va and the 49-% photochlorinated CPE sample in our previous study<sup>10</sup>).

#### Dynamic TGA Experiments

Figures 4 and 6 show the weight loss of the photochlorinated (type Ia) and thermally chlorinated (type Ib) branched polyethylene samples in dynamic TGA experiments. Figure 5 and 7 represent the degradation rates corresponding to the curves in Figures 4 and 6.

As can be seen on Figures 5 and 7 the plots of the degradation rates vs. the chlorine contents by weight reveal two peaks between 180°C and 500°C, depending on the chlorination degree of the CPE samples.

The first peak stands within the 262–272°C interval for the photochlorinated CPE sample (type Ia) and within the 266–288°C interval for the thermal-chlorinated CPE samples (type Ib). Figures 4, 6, and 11 show that, up to 300°C, the hydrochloric acid evolution is responsible for the whole amount of the weight loss of the CPE samples. Therefore we can assign the first peak to the maximum dehydrochlorination rate of the chlorinated sequences present in the CPE chains.

The second peak stands within 400–420°C samples (type Ia) and within 400–418°C for the

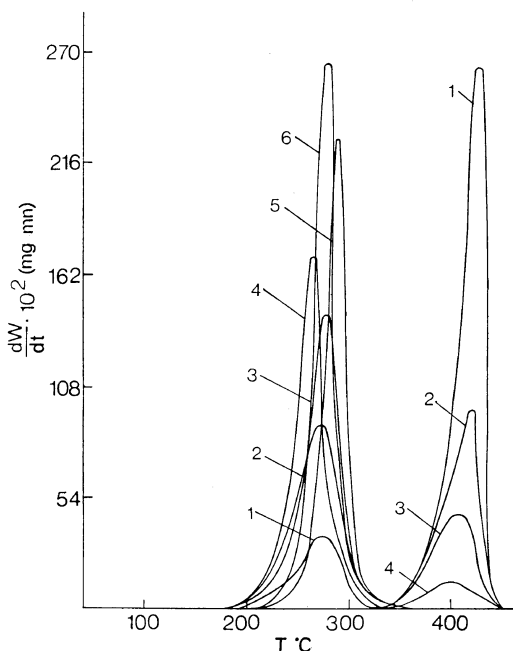


Figure 5. Degradation rates of branched polyethylene samples photochlorinated (20°C) in 1,1,2,2-tetrachloroethane (TCE): 1, 16-% Cl<sub>2</sub>; 2, 46-% Cl<sub>2</sub>; 3, 55-% Cl<sub>2</sub>; 4, 60.5-% Cl<sub>2</sub>; 5, 67.5-% Cl<sub>2</sub>; 6, 73-% Cl<sub>2</sub>.

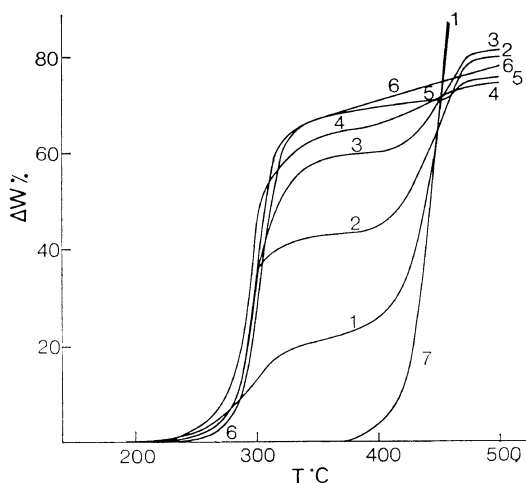


Figure 4. Dynamic TGA (2°C/min) of branched polyethylene samples photochlorinated at 20°C in 1,1,2,2-tetrachloroethane (TCE): 1, 16-% Cl<sub>2</sub>; 2, 46-% Cl<sub>2</sub>; 3, 55-% Cl<sub>2</sub>; 4, 60.5-% Cl<sub>2</sub>; 5, 67.5-% Cl<sub>2</sub>; 6, 73-% Cl<sub>2</sub>; 7, initial LDPE.

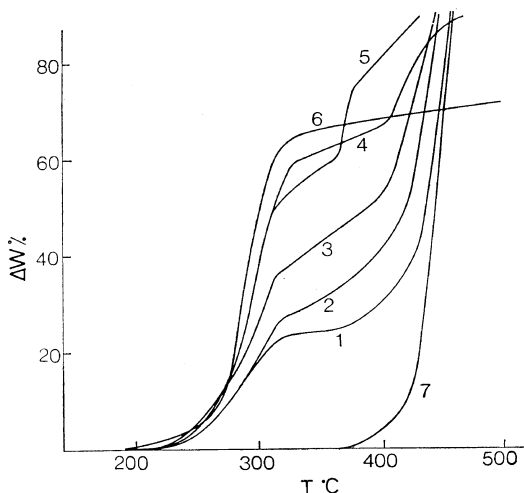
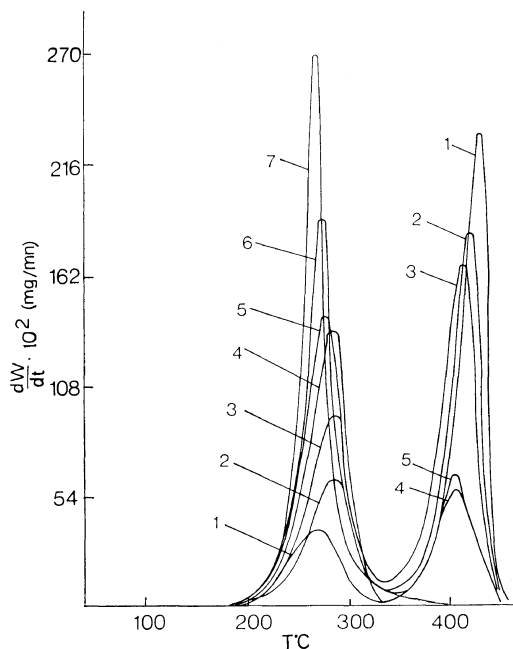


Figure 6. Dynamic TGA (2°C/min) of branched polyethylene samples thermally chlorinated (90°C) in 1,1,2,2-tetrachloroethane (TCE): 1, 24-% Cl<sub>2</sub>; 2, 33-% Cl<sub>2</sub>; 3, 38-% Cl<sub>2</sub>; 4, 54.5-% Cl<sub>2</sub>; 5, 61.5-% Cl<sub>2</sub>; 6, 65-% Cl<sub>2</sub>; 7, initial LDPE.



**Figure 7.** Degradation rates of branched polyethylene samples thermally chlorinated (90°C) in 1,1,2,2-tetrachloroethane (TCE): 1, 24-% Cl<sub>2</sub>; 2, 33-% Cl<sub>2</sub>; 3, 38-% Cl<sub>2</sub>; 4, 54.5-% Cl<sub>2</sub>; 5, 61.5-% Cl<sub>2</sub>; 6, 63-% Cl<sub>2</sub>; 7, 65-% Cl<sub>2</sub>.

thermal CPE samples (type Ib). By comparison to the parent-polymer's behavior in that range of temperature, one can attribute this second peak to the maximum degradation rate corresponding to the evolution of volatile products such as hydrogen gas methane, ethylene, and poorly chlorinated olefines. One must notice that this peak disappears when the CPE sample's chlorine content is higher than 60.5% (type Ia) or 61.5% (type Ib), *i.e.*, when the polyethylene sequences and the  $\beta'_{IV}$  structures (monochloro and dichloropropane or butane) have disappeared.<sup>5</sup>

Figure 8 represents the plot of the maximum dehydrochlorination rate (*viz.*, the first peak value) of the photochlorinated CPE samples (type Ia) against their syndiotacticity-index,  $S$ .<sup>5,6</sup>

The plots of the maximum dehydrochlorination rate of the CPE samples (type Ia and type Ib) *vs.* the ratio, nb CHCl/nb CH<sub>2</sub>, are represented in Figure 9.

These two figures (8 and 9) permit us to show the influence of the microtacticity and the molec-

ular microstructure of CPE samples upon the magnitudes of their dehydrochlorination rates.

As can be seen in Figure 8, up to the 60.5-% chlorine-content value, *i.e.*, till the PVC sequences reach their maximum length,<sup>5</sup> a slight increase of the syndiotacticity-index,  $S$ , leads to a large increase of the maximum dehydrochlorination rate ( $\Delta_r(\text{HCl})/\Delta S \approx 800$ ). When the PVC sequences decrease, from the 60.5-% chlorine-content value, *i.e.*, when the  $\alpha_{II}$  ( $-\text{CHCl}-\text{CHCl}-\text{CHCl}-$  or  $-\text{CH}_2-\text{CHCl}-\text{CHCl}-$ ) and  $\beta_{II}$  ( $-\text{CHCl}-\text{CH}_2-\text{CCl}_2-$ ) structures appear,<sup>5</sup> a large increase of the syndiotacticity-index,  $S$ , leads to only a slight increase of the maximum dehydrochlorination rate ( $\Delta_r(\text{HCl})/S \approx 80$ ).

The first behavior, *i.e.*, the large increase of the maximum dehydrochlorination rate *vs.* a slight increase of the syndiotacticity-index, depends on the microtacticity. Indeed, between  $\varepsilon$ -% and 60.5-% Cl<sub>2</sub>, the PVC sequences increase and the polymeric chains are freed from high steric hindrance,<sup>5</sup> thus the dehydrochlorination occurring on the long PVC syndiotactic sequences *TTTT* can be have like a "zip" mechanism.<sup>16</sup>

The second behavior, *i.e.*, the slight increase of the maximum dehydrochlorination rate *vs.* a large increase of the syndiotacticity, depends on the molecular microstructure.

As can be seen in Figure 9, the maximum dehydrochlorination rate decreases when the  $\alpha_{II}$

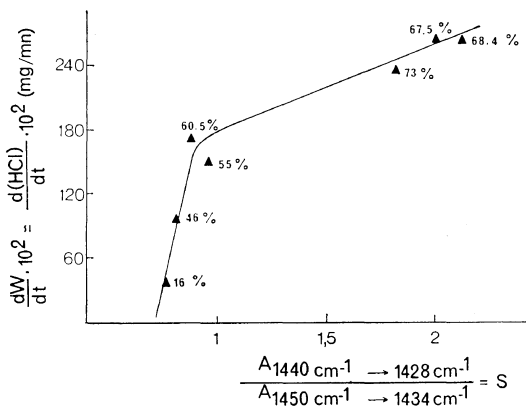


**Figure 8.** Maximum degradation rate *vs.* syndiotacticity-index for branched polyethylene samples photochlorinated (20°C) in 1,1,2,2-tetrachloroethane (TCE). The percentage values represent the chlorine content by weight.

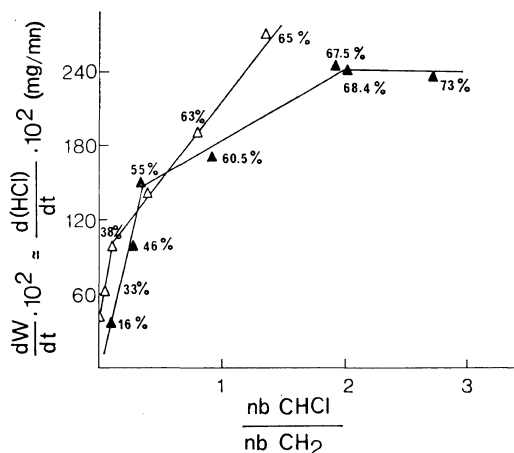


**Figure 9.** Maximum degradation rate vs. the ratio, nb CHCl/nb CH<sub>2</sub>:  $\Delta$ , LDPE thermally chlorinated (90°C) in 1,1,2,2-tetrachloroethane;  $\blacktriangle$ , LDPE photochlorinated (20°C) in 1,1,2,2-tetrachloroethane. The percentage values represent the chlorine content by weight.

and  $\beta_{II}$  structures begin to appear, *i.e.*, when the PVC sequences decrease.<sup>5</sup> Thus, the “zip” process cannot take place on a large scale. At the highest chlorine-content level (73% Cl<sub>2</sub>), the higher a CPE ratio, nb CHCl/nb CH<sub>2</sub>, is the lower is its maximum dehydrochlorination rate (see Table III). This behavior is proof that the  $\alpha_{II}$  ( $-\text{CHCl}-\text{CHCl}-\text{CHCl}-$ ) structure is thermodynamically more stable than the vinyl and vinylidene structures, through the free-radical dehydrochlorination mechanism.<sup>17-19</sup>

#### Isothermal TGA Experiments

The graphs of isothermal degradation versus time (Figure 10) and the plots of the weight loss vs. temperature (Figure 11) show a marked

**Table III.** Maximum dehydrochlorination of various 73% CPE samples

Chlorination medium	Chlorination time, hr	nb CHCl / nb CH <sub>2</sub>	$\frac{dW}{dt} \times 10^2$ , mg/min
UV+TCE, 20°C	4	2.7	2.40
UV+CCl <sub>4</sub> , 20°C	4	3.4	1.68
UV+CCl <sub>4</sub> , 60°C	4	6	1.30

<sup>a</sup> Maximum dehydrochlorination rate.

change in the degradation process for a saturated (73% Cl<sub>2</sub>) CPE sample when the pyrolysis temperature stands in the 270–300°C range. According to the results of Berticat, *et al.*,<sup>4,20-22</sup> a

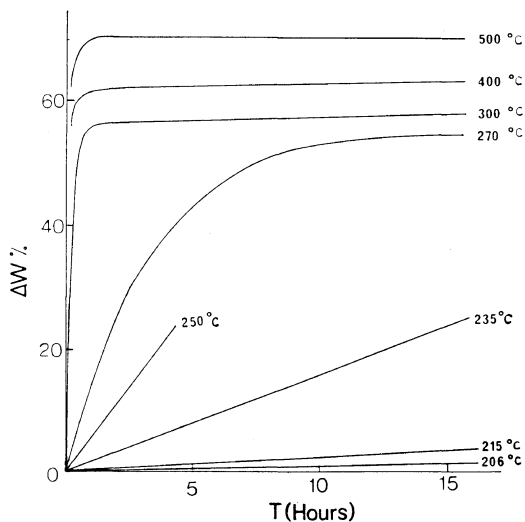


**Figure 10.** Isothermal TGA of the fraction of the highest number-average molecular weight of a (73% CPE) sample produced from a 4-hr photochlorination in CCl<sub>4</sub> at 20°C.

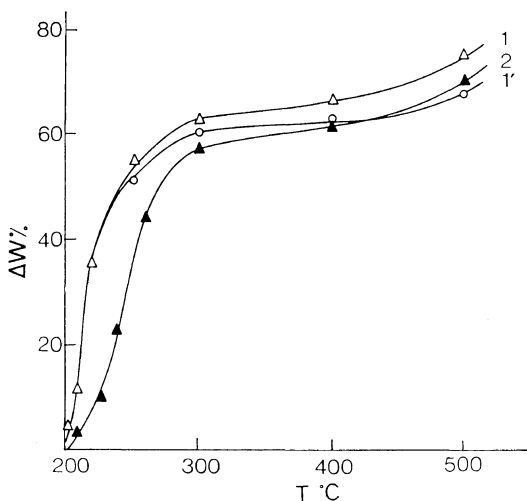


**Figure 11.** 1, pyrolysis in a horizontal oven, model Heraeus; 1' hydrochloric acid evolution; 2, isothermal TGA. Each ( $\blacktriangle$ ) represents a 5-hr degradation at 235°C. Experimental samples were the fraction of the highest number-average molecular weight of a 73% CPE sample produced from a 4 hr photochlorination in CCl<sub>4</sub> at 20°C.



global degradations occur during the pyrolysis process of a 73-% CPE sample or a saturated (73%) chlorinated PVC sample.

Up to about 350°C, intra- and inter-chains dehydrochlorinations, occurring easily by the fluidity exhibited by the material between 200°C and 300°C, take place. They are followed by a rearrangement of the double-bond-containing chains which give polyacenic cycles.

Between 350°C and 800°C, these polyacenic cycles reticulate themselves to give a pregraphitic structure.

In order to show the influence of the molecular microstructure of the 73-% CPE samples upon their dehydrochlorination activation energies, we will consider the first mechanism.

As can be seen in Figure 11, up to 300°C, hydrochloric acid evolution accounts for the entire amount of the weight loss of a saturated (73-% Cl<sub>2</sub>) CPE sample and up to about 270°C (Figure 10) the isothermal weight-loss graphs *vs.* time are straight lines from the intersection of the axes, which indicates that the dehydrochlorination mechanism is a zero-order one. Thus Arrhenius' plots can be drawn for a series of saturated (73%) CPE samples (Figure 12) to calculate their global activation energies of dehydrochlorination.

The activation energies values ( $E_a$ ) are listed in Table IV, along with the main characteristics of the highest number-average molecular weight

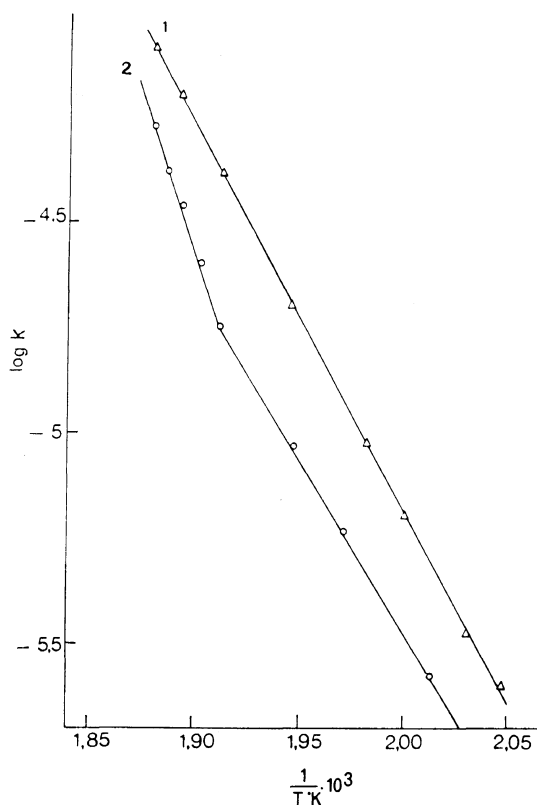


Figure 12. Arrhenius' plots: 1, nb CHCl/nb CH<sub>2</sub> < 4; 2, nb CHCl/nb CH<sub>2</sub> ≥ 4.

Table IV. Fractions of the highest number-average molecular weight of the 73-% CPE samples

Initial polymers	Chlorination medium	Chlorination temperature, °C	Chlorination time, hr	% $\overline{HM}_n^a$	Cl/C ( $\overline{HM}_n$ ) <sup>a</sup>	$\overline{DP}_n$ ( $\overline{HM}_n$ ) <sup>a</sup>	$P = \frac{\overline{M}_w}{\overline{M}_n}$ ( $\overline{HM}_n$ ) <sup>a</sup>	Den- sity	nbCHCl/nbCH <sub>2</sub>	$E_a$ , kcal	$\frac{S_{HH}}{S_{HCl}} = \frac{A_{615}}{A_{685}}$
LDPE	UV+CCl <sub>4</sub>	20	4	75	1	537	2.13	1.6650	3.4	45	0.11
LDPE	UV+CCl <sub>4</sub>	20	6	70	1	400	—	1.6758	3.5	45	0.28
LDPE	UV+CCl <sub>4</sub>	20	8	65	1	289	—	1.6844	3.7	45	0.27
LDPE	UV+CCl <sub>4</sub>	40	4	—	1	515	2.4	1.6720	4.5	35 70	0.31
LDPE	UV+CCl <sub>4</sub>	60	4	61	1	—	2.2	1.6772	6	35 70	0.37
LDPE	UV+TCE	20	4	75	1	1040	4	1.6615	2.7	45	0
HDPE	UV+CCl <sub>4</sub>	20	4	90	1	516	3.25	1.6616	3.4	45	0.35
HDPE	UV+CCl <sub>4</sub>	20	6	86	1	505	—	1.6644	3.4	45	0.28
HDPE	UV+CCl <sub>4</sub>	20	8	86	1	516	—	1.6640	3.4	45	0.26
HDPE	UV+CCl <sub>4</sub>	40	4	90	1	—	—	1.6622	3.7	45	0.28
HDPE	UV+CCl <sub>4</sub>	60	4	87	1	—	2.6	1.6610	4	35 60	0.34

<sup>a</sup>  $\overline{HM}_n$ , fractions of the highest number-average molecular weight of the 73-% CPE samples.

## Chlorinated Polyethylene. III.

( $\overline{HM}_n$ ) fractions of the 73-% CPE samples, *viz.*, polydispersity,  $\overline{DP}_n$ , density, nb CHCl/nb CH<sub>2</sub>, and conformation:  $S_{HH}/S_{HC}$  or  $S_{HH}/S_{HCl}$ .<sup>6</sup>

One can notice that only the variations of the ratio, nb CHCl/nb CH<sub>2</sub>, have an influence upon the  $E_a$  values. When this ratio value is less than 4, a saturated CPE sample has a unique global dehydrochlorination  $E_a$  of about 45 kcal. When this ratio stands between 4 and 6 there are two global dehydrochlorination  $E_a$ : the first one, about 35 kcal, rules the dehydrochlorination process up to 244–250°C; the second, about 60 to 70 kcal, acts above this interval of temperature (247–250°C) (Figure 12).

It is important to remark that, according to Oswald and Kubu,<sup>1</sup> the  $T_g$  of polyethylene dichloride (—CHCl—CHCl—CHCl—)<sub>n</sub> is at least equal to 226°C. This estimate have been obtained by using the well-known empirical equation applied to random copolymers:<sup>24</sup>

$$T_g = \sum M_i T_{g_i}$$

where

$M_i$ : the mole fraction of the *i*th component,  
 $T_g$ : the glass temperature of the copolymer in degrees Kelvin,

$T_{g_i}$ : the glass temperature of the homopolymer of the *i*th component.

The value 226°C is undoubtedly below the real one because these authors<sup>1</sup> have not taken into account the contribution of the vinylidene chloride and trichloroethylene units.

Moreover, Murayama and Amagi<sup>23</sup> demonstrated that head-to-head poly(vinylidene chloride) (H-H-PVDC) is less thermally stable than head-to-tail PVC or H-H-PVC within the 200–260°C range.

Thus, taking into account these results<sup>1,23</sup> and listing them together with the microstructural NMR studies,<sup>5,10</sup> the Dupont 942 TMA experiments and the TGA results, and assuming that the dehydrochlorination process starts after the concerned structures have gone into full motion, *i.e.*, when their main second-order transition temperature is exceeded, one can attribute the

Table Va. Branched polyethylene samples photochlorinated in 1,1,2,2-tetrachloroethane at 20°C, Type Ia

$T$ -% Cl <sub>2</sub>	$\frac{\text{nb CHCl}}{\text{nb CH}_2}$	$T^a$ , °C	Structures responsible for the second-order transition	$T^a$ , °C	$\frac{\text{nb CHCl}}{\text{nb CH}_2}$	$T$ -% Cl <sub>2</sub>
16	0.111	36 <sup>+b</sup>	—CH <sub>2</sub> —CH <sub>2</sub> (short vinyl sequences in amorphous phase) CH <sub>2</sub> —CH <sub>2</sub> —	33 <sup>+b</sup>	—	19.5
		103	motions in partly chlorinated crystalline-phase			
46	0.266	48 <sup>+b</sup>	—CH <sub>2</sub> —CHCl—CH <sub>2</sub> —CCl <sub>2</sub> —CH <sub>2</sub> —CCl <sub>2</sub> —CH <sub>2</sub> —CHCl— CH <sub>2</sub> —	66	0.316	55
		71	—CH <sub>2</sub> —CH <sub>2</sub> —long vinyl sequences—CH <sub>2</sub> —CH <sub>2</sub> —	78 <sup>+</sup>		
		90	motions in partly chlorinated crystalline-phase			
60.5	0.9	76 <sup>+b</sup>	long vinyl sequences			
		88	motions in partly chlorinated crystalline-phase			
		76	vinyl sequences	78		
67.5	1.88	108 <sup>+b</sup>	—CHCl—CHCl—CHCl—CH <sub>2</sub> —CHCl—CH <sub>2</sub> —CHCl— CHCl—	137 <sup>+b</sup>	1.98	68.4
		148	—CHCl—CHCl—CHCl—CH <sub>2</sub> —CCl <sub>2</sub> —CHCl—CHCl— CHCl—	150		

<sup>a</sup> Temperatures of the second-order transitions.

<sup>b</sup> The plus-marked transitions represent the glass transitions.

**Table Vb.** Branched polyethylene samples thermally chlorinated in 1,1,2,2-tetrachloroethane at 90°C, Type Ib

$T-\%$ $\text{Cl}_2$	$\frac{\text{nb CHCl}}{\text{nb CH}_2}$	$T^a, ^\circ\text{C}$	Structures responsible for the second-order transition	$T^a, ^\circ\text{C}$	$\frac{\text{nb CHCl}}{\text{nb CH}_2}$	$T-\%$ $\text{Cl}_2$
24	$\epsilon$	32 <sup>+b</sup>	$(-\text{CH}_2-)_8\text{CCl}_2-\text{CH}_2-\text{CCl}_2-\text{CH}_2(-\text{CH}_2-\text{CH}_2-)_8$			
		56	<i>motions in partly chlorinated crystalline-phase</i>			
			$-\text{CHCl}-\text{CH}_2-\text{CH}_2-\text{CH}_2-\text{CCl}_2-\text{CH}_2-\text{CCl}_2-\text{CH}-\text{CHCl}-$	-12 <sup>+b</sup>	0.07	33
54.5	0.38	60 <sup>+b</sup>	$-\text{CHCl}-\text{CH}_2-\text{CH}_2-(\text{short vinyl sequences})-\text{CH}_2-\text{CH}_2-\text{CCl}_2-$			
61.5	0.44	55 <sup>+b</sup>	$-\text{CCl}_2-\text{CH}_2-\text{CH}_2-(\text{maximum length of the vinyl sequences})-\text{CH}_2-\text{CH}_2-\text{CHCl}$	58		
			<i>long vinyl sequences</i>	70 <sup>+b</sup>	1.31	65
			$-\text{CHCl}-\text{CHCl}-\text{CH}_2-\text{CHCl}-\text{CH}_2-\text{CHCl}-\text{CHCl}-$	102		

<sup>a</sup> Temperatures of the second-order transition.

<sup>b</sup> The plus-marked transitions represent the glass transitions.

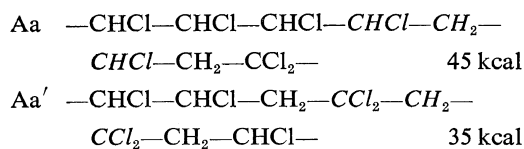
**Table Vc.** Linear polyethylene samples thermally chlorinated in 1,1,2,2-tetrachloroethane at 110°C, Type Ic

$T-\%$ $\text{Cl}_2$	$\frac{\text{nb CHCl}}{\text{nb CH}_2}$	$T^a, ^\circ\text{C}$	Structures responsible for the second-order transitions	$T^a, ^\circ\text{C}$	$\frac{\text{nb CHCl}}{\text{nb CH}_2}$	$T-\%$ $\text{Cl}_2$	
6	$\epsilon$	10 <sup>+b</sup>	$(-\text{CH}_2-\text{CH}_2-)_8-\text{CCl}_2-\text{CH}_2-\text{CH}_2-\text{CCl}_2-(\text{CH}_2-\text{CH}_2-)_8$				
		104	<i>motions in partly chlorinated crystalline-phase</i>				
			$-\text{CHCl}-\text{CH}_2-\text{CH}_2-\text{CCl}_2-\text{CH}_2-\text{CCl}_2-\text{CH}_2-\text{CH}_2-\text{CHCl}-$	0 <sup>+b</sup>	0.114	41	
		52	$-\text{CCl}_2-\text{CH}_2-\text{CH}_2-(\text{short vinyl sequences})-\text{CH}_2-\text{CHCl}-$				
56	0.483	68 <sup>+b</sup>	<i>long vinyl sequences</i>	76 <sup>+b</sup>			
			90	$-\text{CHCl}-\text{CHCl}-(\text{short vinyl sequences})-\text{CHCl}-\text{CHCl}-$	94	1.27	61.7
				$-\text{CHCl}-\text{CHCl}-\text{CHCl}-\text{CH}_2-\text{CHCl}-\text{CHCl}-\text{CHCl}-\text{CHCl}-$	130		
		75	<i>vinyl sequences</i>	80 <sup>+b</sup>			
67	2.66	160 <sup>+b</sup>	$-\text{CHCl}-\text{CHCl}-\text{CHCl}-\text{CH}_2-\text{CHCl}-\text{CH}_2-\text{CHCl}-\text{CHCl}-\text{CHCl}-$	128	1.98	64	
			176	$-\text{CHCl}-\text{CHCl}-\text{CHCl}-\text{CHCl}-\text{CH}_2-\text{CCl}_2-\text{CHCl}-\text{CHCl}-\text{CHCl}-$	160		

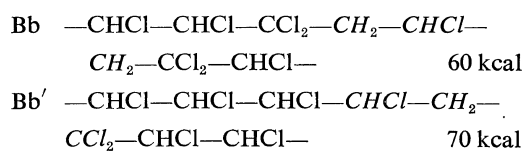
<sup>a</sup> Temperatures of the second-order transitions.

<sup>b</sup> The plus-marked transitions represent the glass transitions.

35-kcal and 45-kcal  $E_a$  to the global dehydrochlorination activation energy of the sequences (type A) below:



and the 60-kcal and 70-kcal  $E_a$  to sequences (type B) below:



If we consider that the initiation rate rules the dehydrochlorination rate, the italic-written segments of the above sequences (types A and B) can be regarded as the initiation sites of the degradation process.

#### CONCLUSION

The isothermal TGA results confirm the assumptions made during the discussion about the second-order transitions, *viz.*, the temperatures at which the sequences of type A go into motion are lower than those of the sequence of type B.

We can now assign the different second-order transitions, observed with the Dupont 942 TMA experiments, to the molecular structures which can be regarded as responsible for them (Tables V). A portion of these different structures have been written in italic, in order to point out their particular contribution to the second-order transition. When a CPE sample has many second-order transitions, the responsible structures can belong either to the same polymeric chain; and therefore they are each from widely separated other; or they can belong to distinct polymeric chains. The values of the ratio,  $\text{nb CHCl}/\text{nb CH}_2$ , in Tables V give a rough estimate of the chlorinated chains' length.

Our previous study<sup>10</sup> dealing with the dynamic mechanical properties of the CPE samples studied here confirms these structural attributions.

#### REFERENCES

- H. J. Oswald and E. T. Kubu, *SPE, Trans.*, **3**, 168 (1963).
- Vaino A. Erä and J. Johan Lindberg, *J. Polym. Sci., Part A-2*, **10** 937 (1972).
- Ismat. A. Abu Isa, *ibid.*, *Part A-2*, **10**, 881 (1972).
- N. Saglio, P. Berticat, and G. Vallet, *J. Appl. Polym. Sci.*, **16**, 2991 (1972).
- B. M. Quenum, P. Berticat, and G. Vallet, *Polymer J.*, **7**, 287 (1975).
- B. M. Quenum, P. Berticat, and G. Vallet, *ibid.*, **7**, 277 (1975).
- B. M. Quenum, P. Berticat, and Q. T. Pham, *Eur. Polym. J.*, **7**, 1527 (1971).
- B. M. Quenum, P. Berticat, and Q. T. Pham, *ibid.*, **9**, 777 (1973).
- G. Humbert, B. M. Quenum, P. Berticat, Q. T. Pham, and G. Vallet, *Makromol. Chem.*, **175**, 1597 (1974).
- G. Humbert, B. M. Quenum, P. Berticat, and G. Vallet, *ibid.*, **175**, 1611 (1974).
- T. F. Schatski, *J. Polym. Sci.*, **57**, 496 (1962).
- R. F. Boyer, *Rubber Chem. Tech.*, **36**, 1303 (1963).
- W. W. Wendlandt, "Thermal Methods of Analysis, Interscience, New York, N.Y., 1964.
- A. Guyot and M. Bert, *J. Appl. Polym. Sci.*, **17**, 753 (1973).
- J. D. Hoffman and B. M. Axilrod, *J. Res. Nat. Bur. Stds*, **54**, 357, RP 2598 (1955).
- J. Millan, M. Caransa, and J. Gusman, IUPAC Symposium on Macromolecules, Helsinki 1972, Preprint IV, 21, Vol. 5.
- E. J. Arlman, *J. Polym., Sci.*, **12**, 543 (1959).
- B. Baum and L. H. Wartman, *ibid.*, **28**, 537 (1968).
- B. Baum and M. Thallmaier, *Kunststoffe*, **56**, 80 (1966).
- P. Berticat, J. J. Bejat, and G. Vallet, *J. Chim. Phys.*, **67**, 164 (1970).
- P. Berticat, J. J. Bejat, *ibid.*, **67**, 170 (1970).
- P. Berticat, J. J. Bejat, J. F. May, and G. Vallet, *ibid.*, **67**, 176 (1970).
- N. Murayama and Y. Amagi, *Polym. Letters*, **4**, 119 (1966).
- A. V. Tobolsky, "Properties and Structure of Polymers, Wiley and Sons, New York, N.Y., 1960.